

# Input and state estimation for earthquake-excited building structures using acceleration measurements

By

Sdiq Anwar Taher

Submitted to the graduate degree program in Civil Engineering and the Graduate Faculty of the  
University of Kansas in partial fulfillment of the requirements for the degree of Master of  
Science in Civil Engineering.

---

Chairperson: Prof. Jian Li

---

Prof. Huazhen Fang

---

Prof. Caroline Bennett

Date Defended: May 2, 2018

The thesis committee for Sdiq Anwar Taher certifies that this is the  
approved version of the following thesis:

**Input and state estimation for earthquake-excited building structures  
using acceleration measurements**

---

Chair: Prof. Jian Li

Date Approved: May 2, 2018

## Abstract

Estimating both state and ground input for earthquake-excited building structures using a limited number of absolute acceleration measurements is critical to post-disaster damage assessment and structural evaluation. Input estimation in this case is particularly challenging due to the lack of direct feedthrough term, which renders the system weakly observable for its input. Hence, input estimation in this scenario is sensitive to modeling error and measurement noise. In this thesis, a two-step strategy is proposed to estimate both state (displacement and velocity) and ground input using a limited number of absolute acceleration measurements for building structures. First, the ground input is estimated by solving a least squares problem with Tikhonov regularization and Bayesian inference. In the second step, floor states are estimated using Kalman filter with input obtained from the first step, the least squares with Tikhonov regularization and Bayesian inference. The proposed strategy was numerically and experimentally evaluated based on shear-type building structures.

## Acknowledgements

First of all, I would like to sincerely thank my major sponsor, the Higher Committee for Education Development in Iraq (HCED) for providing me with financial support to complete my MS degree at the University of Kansas.

I would like to express my sincere gratitude to my advisor Professor Jian Li for his advice, continuous support, and encouragement during my MS study. He introduced me to the field of structural health monitoring, and shared his extensive knowledge with me. I would say that it is my greatest honor to be his student, and he is an excellent advisor. His patience and effort during revising the research will not be forgotten. Without his help, support, and advice, this thesis could not be done. Again, I'm grateful to him forever.

I wish to express my gratitude to my MS committee members, Professor Huazhen Fang, and Professor Caroline Bennett, for viewing this thesis. I would also say that Professor Huazhen Feng shared his extensive knowledge with me. I learned from him a lot in field of optimal estimation. His advice and help during my MS study will not be forgotten. Therefore, I would be also grateful to him. Special thanks go to Professor Caroline Bennett for accepting my invitation to be a committee member. I would also say that I learned from her a lot in her class, design of steel structure. Therefore, I'm grateful to her.

I also sincerely thank international student service at the University of Kansas for their support and help, and my friend Abdulaziz Almarshad for sharing his experimental data with us.

In that journey, my parents have been my greatest supporter for me. Therefore, I would like to express my deepest thanks to mother and father, Zulaikha Abdullah and Anwar Taher. Thanks go to my sisters and brothers. I would also have special thanks to my younger brother

Hoger Taher for his help and support during my MS study. Finally, there are so many people that helped me during my MS study, who I did not name here. I would say thank you so much.

## Table of Contents

LIST OF FIGURES .....	ix
LIST OF TABLES .....	xi
Chapter 1 : INTRODUCTION.....	1
1.1 Literature review .....	1
1.1.1 Kalman filter-based approach.....	2
1.1.2 Offline approaches .....	4
1.2 Outline of the thesis .....	5
Chapter 2 : MATHEMATICAL FORMULATION .....	7
2.1 Equation of motion .....	7
2.2 State space formulation.....	8
2.2.1 Continuous-time state space model .....	8
2.2.2 Discrete-time state space model.....	9
2.3 Proposed strategy .....	10
2.3.1 Input Reconstruction.....	10
2.3.2 State Estimation .....	11
2.4 The proposed strategy for joint input-state estimation for earthquake-excited building structures.....	12
2.5 Online state and input estimation.....	13
2.6 Observability of system input .....	14

2.7 Summary .....	14
Chapter 3 : NUMERICAL INVESTIGATION .....	16
3.1 Numerical model.....	16
3.2 Stationary ground input.....	19
3.2.1 Input estimation results .....	19
3.2.2 State estimation results .....	20
3.2.3 Input-state estimation under different level of measurement noise and modeling errors .....	22
3.3 Joint state-input estimation based on a non-stationary earthquake input .....	23
3.3.1 Input estimation results .....	23
3.3.2 State estimation results .....	25
3.4 Comparative study .....	26
3.5 Summary .....	28
Chapter 4 : EXPERIMENTAL INVESTIGATION .....	29
4.1 Laboratory model and measurement setup .....	29
4.2 Proposed strategy and system identification based on experimental study .....	31
4.3 Joint input-state estimation based on earthquake input .....	32
4.3.1 Ground input identification results .....	33
4.3.2 State estimation results .....	34
4.4 Summary .....	36

Chapter 5 : CONCLUSIONS.....	37
5.1 Conclusions and main contributions.....	37
5.2 Recommendations for further work.....	39
REFERENCES .....	41



## LIST OF FIGURES

Figure 2.1: Flowchart of the proposed two-step strategy .....	13
Figure 3.1: A four-story shear-type building .....	17
Figure 3.2: Ground input estimation with 12% measurement noise and 5% modeling error.....	18
Figure 3.3: State (relative displacement and velocity) estimation with 12% measurement noise and 5% modeling error.....	21
Figure 3.4: Estimated absolute acceleration at the unmeasured (3rd) floor in case 2, with 12% measurement noise and 5% modeling error. (Amplitude error = 9%, phase error = 5.1%, FDE = 14.1%).....	22
Figure 3.5: The frequency domain errors (FDE) of (a) input estimation, and (b) displacement estimation at the 4th floor under different levels of measurement noise and modeling error .....	22
Figure 3.6: Non-stationary ground input estimation with 12% measurement noise and 5% modeling error.....	24
Figure 3.7: State (relative displacement and velocity) estimation with 12% measurement noise and 5% modeling error.....	26
Figure 3.8: Estimated absolute acceleration at the unmeasured (3rd) floor in case 2, with 12% measurement noise and 5% modelling error. (Amplitude error = 11.2%, phase error = 6.1%. FDE = 17.3%).....	26
Figure 3.9: Non-stationary ground input estimations with 12% measurement noise and 5% modeling error.....	27
Figure 4.1: The six-story laboratory frame structure and measurement setup .....	30
Figure 4.2: Time history of the ground input estimation (Top), and detail of the time history (bottom). (Amplitude error = 19.4 %, phase error = 9.1%, FDE = 28.5%).....	33

Figure 4.3: Time history of the estimated relative displacement at floor 6th (left), and detail of the time history (right). (Amplitude error = 3.9 %, phase error = 7.9 %, FDE = 11.9%) .....	34
Figure 4.4: Time history of the estimated relative velocity at floor 6th (left), and detail of the time history (right) .....	35
Figure 4.5: Time history of the absolute acceleration estimation at floor 4th (left), and detail of the time history (right). (Amplitude error = 15 %, phase error = 15.1 %, FDE = 30.1%) .....	35

## LIST OF TABLES

Table 3.1: Structural parameters .....	17
Table 3.2: Two cases with different sensing information.....	17
Table 4.1: Experimental natural frequencies and damping ratios for the six-story laboratory structure.....	32

## **Chapter 1 : INTRODUCTION**

Earthquakes pose great threats to civil engineering structures in seismic zones, including building structures. Post-earthquake structural assessment is critical to support informed decision-making and safe operation. Interstory drift is one of the most commonly applied performance index for assessment of building structures. However, since floor displacements are not easily measurable in practice, various indirect methods based on floor acceleration data have been developed for estimating floor displacements. For example, the Kalman Filter, a model-based estimation method, can be used to estimate unmeasured states (e.g. displacements). In this case, input information needs to be known. However, ground inputs to building structures are often not measurable in many cases in practice. For example, most earthquake ground motions have been typically recorded using Strong Motion Instrumentation. Examples of the recorded ground motions during earthquake include the 1989 Loma Prieta earthquake, and the 1994 Northridge earthquake in California, the 1999 Chi-Chi earthquake in Taiwan, and the 2011 Tohoku earthquake in Japan. However, for building structures, these recorded ground motions may not represent the actual input to the building and may vary from one place to another as their accuracy often depends on several factors including the soil condition, number of stations instrumented, etc. [1]. Therefore, it is still challenging to obtain state and ground input for earthquake-excited building structures.

### **1.1 Literature review**

Some efforts have been devoted to reconstruct input based on measured relative structural responses and full response measurements. For example, for the case of earthquake-excited building structures, Li et al. [2] developed a statistical average algorithm to estimate structural

parameters and ground motion using the equation of motion in relative coordinates, for which relative acceleration measurements are therefore required. Zhao et al. [3,4] presented a hybrid identification method under absolute coordinates to identify structural parameters and ground motion of an multi-story building based on the assumption that all structural responses are known, including displacements, velocities, and accelerations. However, since accelerations are measured in absolute coordinates and full response measurement maybe impractical, the applicability of the aforementioned methods for ground input estimation would be limited.

#### 1.1.1 Kalman filter-based approach

In recent years, online input-state estimation considering uncertainties in the state variables and measurements, referred to as the combined deterministic-stochastic methods, has been explored. Various Kalman filter-based approaches [5-18] were presented to identify both states and inputs together for linear systems in cases of with and without direct feedthrough. Lourens et al. [5] proposed an augmented Kalman filter algorithm for force identification in which unknown forces are incorporated in the state vector in order to identify them together. The algorithm was experimentally investigated by estimating input and state for a steel beam. When only acceleration measurements were used, the algorithm was unstable [6] and the augmented system matrix has unobservability issue [5, 12]. Therefore, dummy-measurement in [6] and heterogeneous structural measurements, strain and acceleration, in [7] in addition to acceleration measurements were included in the input and state estimation to tackle the problem. Gillijns and De Moor [8] developed a Kalman filter-based joint input and state estimation algorithm for linear discrete-time systems with direct feedthrough. The algorithm was later applied in structural dynamics using a limited number of acceleration measurements and reduced-order models,

examined through a numerical example, a laboratory experiment, and in situ experiment on a footbridge [9]. Maes et al. [10, 11] presented further improvement in [9] by incorporating the displacement in addition to acceleration measurements and the effect of unknown stochastic force, e.g. wind loads. The improvement was confirmed to estimate force and response using a numerical simulation on a cantilever beam and in situ experiment on a footbridge. Furthermore, Azam, et al. [12] developed a dual Kalman filter approach (DKF) for linear systems with direct feedthrough. The approach was applied to identify state and input from acceleration measurements in numerical simulations.

However, for earthquake-excited building structures, the fact that floor responses are measured in terms of absolute accelerations renders the system without direct feedthrough, leading to weak observability of the system input. Several Kalman filter-based approaches have been proposed for joint input-state estimation of systems without direct feedthrough [13-18]. For example, a Kalman filter-based joint input and state estimation algorithm for linear discrete-time systems (Gillijns Algorithm) was proposed by Gillijns and De Moor [13]. The algorithm was designed to estimate input and state for systems without direct feedthrough. Tuan et al. [15] proposed the Kalman filter and recursive least-squares algorithm for input estimation, in which full response measurements were required. The algorithm was applied by Liu et al. [16] and Ma et al. [17] to identify the input force for a cantilever plate and beam through experimental testing and numerical simulations. Wu et al. [18] later used Tuan's algorithm to estimate the soil-structural interaction forces of soil-pile interaction during shake table tests. Although there have been some Kalman filter-based approaches for joint input-state estimation of systems without direct feedthrough, the weak observability of system input makes the estimation sensitive to measurement noise, modeling error, and incomplete measurements.

### 1.1.2 Offline approaches

On the other hand, an offline input estimation strategy based on the least squares method with Tikhonov regularization [19-21] and Bayesian inference [22, 25] has been widely used to tackle the ill-posed inverse problem. For example, average acceleration discrete algorithm through state space form [19], explicit form of the Newmark- $\beta$  method [20], and state space formulation [21] were applied for estimation of unknown inputs using Tikhonov regularization. Feng et al. [22] presented identification of parameter and vehicle loads using Bayesian inference [24, 25]. The approach presented in [22] was verified utilizing numerical examples on a single-span simply supported bridge and a three-span continuous bridge. It is noted that the Bayesian inference, compared with other approaches, e.g. L-curve method [26], can effectively find optimal regularization parameters for large values of the matrix size [22, 23]. Generally, these methods provided satisfactory results of external input estimations including sinusoidal, impact and moving forces.

The research work in the literature indicates that state and input estimation for earthquake-excited building structures using a limited number of absolute acceleration measurements have received less attention. This research is focused on identification of both state and ground input using a limited number of absolute acceleration measurements for earthquake-excited building structures. A two-step strategy is proposed. First, the ground input is estimated by solving a least squares problem with Tikhonov regularization and Bayesian inference. Second, Kalman filter is applied to estimate the floor displacements using the estimated ground input and absolute floor acceleration measurements.

## 1.2 Outline of the thesis

The purpose of this thesis is to estimate both state and input for system without direct feedthrough, e.g. system model of earthquake-excited building structures, using incomplete measurements. The thesis is arranged as follows:

Chapter 2: The state space model for linear systems which is widely used in the model-based input identification in time domain is explained for earthquake-excited building structures. The mathematical formulation of the proposed strategy to estimate state, input, and response at unmeasured location is presented in two steps. In addition, a part of the chapter deals with the Gillijns Algorithm for system without direct feedthrough [13] and the observability of system input in order to highlight existing methods for input and state estimation in case of systems without direct feedthrough and the ill-conditioned problem.

Chapter 3: In this chapter, the effectiveness and robustness of the proposed strategy under a stationary and non-stationary ground input is verified through numerical simulation of a shear-type building structure by considering various noise levels, modelling errors and incomplete measurements. The accuracy of the results obtained from the proposed strategy is shown using the frequency domain error (FDE) [30]. The effectiveness of the proposed strategy is further illustrated through comparison with an online methodology, the Gillijns Algorithm, considering both complete and incomplete measurements.

Chapter 4: Experimental investigation on the proposed strategy is carried out using a scaled six-story laboratory frame structure subjected to a non-stationary ground input, a ground motion recorded from the 1994 Burbank earthquake. Firstly, the accelerometers were attached to the floors to obtain absolute acceleration measurements, whereas the reference displacement at top floor was obtained through computer vision technique using a smartphone camera. A limited



number of absolute accelerations obtained from accelerometers are used in the estimation of states and the ground input. By comparing the estimated input and states with the measured ones, the accuracy of the proposed strategy is confirmed.

Chapter 5: This chapter presents the conclusion of the research. Moreover, future work is also discussed.

## Chapter 2 : MATHEMATICAL FORMULATION

This chapter presents the mathematical formulations for the research. In particular, an offline strategy is presented to estimate input and state for systems without direct feedthrough, e.g. system model of earthquake-excited building structures. The strategy consists of a least squares method with Tikhonov regularization and Bayesian inference for input and the Kalman filter for state and response estimations. To compare the proposed method with existing online methods for input and state estimation for system without direct feedthrough, the online algorithm proposed in [13] is introduced here, which will be applied in a later chapter. Furthermore, the observability of system input is discussed at the end of the chapter.

This chapter is arranged as follows: Section 2.1 introduces the equation of motion for earthquake-excited building structures in relative coordinates; Section 2.2 explains the state space formulations; Section 2.3 and Section 2.4 presents the proposed strategy to estimate state and input for systems without direct feedthrough; Section 2.5 describes an online input and state estimation algorithm; Section 2.6 illustrates the observability of the system input; Section 2.7 provide the summary of the chapter.

### 2.1 Equation of motion

The equation of motion in the relative coordinates for earthquake-excited building structures can be written as:

$$\mathbf{M}\ddot{\mathbf{u}}_r(t) + \mathbf{C}\dot{\mathbf{u}}_r(t) + \mathbf{K}\mathbf{u}_r(t) = -\mathbf{M}\mathbf{L}\ddot{\mathbf{u}}_g(t) \quad (1)$$

Where  $\mathbf{M}, \mathbf{C}$ , and  $\mathbf{K} \in \mathbb{R}^{n \times n}$  are the building mass, damping, and stiffness matrices, respectively.  $\ddot{\mathbf{u}}_g(t) \in \mathbb{R}$  is a ground acceleration input vector,  $\mathbf{L} \in \mathbb{R}^n$  is the ground input

selection vector, in which  $\mathbf{L}$  is equal to  $[1 \ 1 \ \dots \ 1]^T$ , and  $\ddot{\mathbf{u}}_r, \dot{\mathbf{u}}_r$ , and  $\mathbf{u}_r \in \mathbb{R}^n$  are the relative acceleration, velocity, and displacement vectors, with  $n$  the number of degree of freedoms.

## 2.2 State space formulation

### 2.2.1 Continuous-time state space model

Eq. (1) can be re-written as a first-order continuous-time state space form:

$$\dot{\mathbf{x}}(t) = \mathbf{A}_c \mathbf{x}(t) + \mathbf{B}_c \ddot{\mathbf{u}}_g(t) \quad (2)$$

with

$$\mathbf{A}_c = \begin{bmatrix} \mathbf{0} & \mathbf{I} \\ -\mathbf{M}^{-1}\mathbf{K} & -\mathbf{M}^{-1}\mathbf{C} \end{bmatrix}, \text{ and } \mathbf{B}_c = \begin{bmatrix} \mathbf{0} \\ -\mathbf{L} \end{bmatrix} \quad (3)$$

$\mathbf{x}(t) \in \mathbb{R}^{n_s}$  is the state vector,  $\mathbf{A}_c \in \mathbb{R}^{n_s \times n_s}$  and  $\mathbf{B}_c \in \mathbb{R}^{n_s \times 1}$  are the system matrix and input vector, respectively, and  $\mathbf{I} \in \mathbb{R}^{n \times n}$  is identity matrix, with  $n_s$  the number of states. The state vector  $\mathbf{x}(t)$  contains the relative displacement and velocity:

$$\mathbf{x}(t) = \begin{bmatrix} \mathbf{u}_r(t) \\ \dot{\mathbf{u}}_r(t) \end{bmatrix} \quad (4)$$

In general, the measurement equation  $\mathbf{y}(t)$  can be written as a linear combination of acceleration, velocity, and displacement vectors:

$$\mathbf{y}(t) = \mathbf{S}_a \ddot{\mathbf{u}}_r(t) + \mathbf{S}_v \dot{\mathbf{u}}_r(t) + \mathbf{S}_d \mathbf{u}_r(t) \quad (5)$$

$\mathbf{S}_a, \mathbf{S}_v$ , and  $\mathbf{S}_d \in \mathbb{R}^{n_d \times n}$  are the output influence matrix for acceleration, velocity, and displacement, respectively, giving the knowledge of measurement locations, with  $n_d$  the number of measurements. If relative acceleration responses are measured, the measurement equation  $\mathbf{y}(t)$  can be rewritten as  $\mathbf{y}(t) = \mathbf{S}_a \ddot{\mathbf{u}}_r$ . Thus, the measurement equation can be formulated as:

$$\mathbf{y}(t) = \mathbf{C}_c \mathbf{x}(t) + \mathbf{D}_c \ddot{\mathbf{u}}_g(t) \quad (6)$$

with

$$\mathbf{C}_c = [-\mathbf{S}_a \mathbf{M}^{-1} \mathbf{K} \quad -\mathbf{S}_a \mathbf{M}^{-1} \mathbf{C}] , \text{ and } \mathbf{D}_c = [-\mathbf{S}_a \mathbf{L}] \quad (7)$$

$\mathbf{C}_c \in \mathbb{R}^{n_d \times n_s}$  and  $\mathbf{D}_c \in \mathbb{R}^{n_d \times 1}$  are the output matrix and direct feedthrough vector, respectively. In the case of earthquake-excited building structures, the absolute acceleration responses are measured, and the direct feedthrough vanishes. Hence the measurement equation  $\mathbf{y}(t)$  becomes:

$$\mathbf{y}(t) = \mathbf{C}_c \mathbf{x}(t) \quad (8)$$

in which the output of  $\mathbf{y}(t)$  are absolute acceleration responses.

### 2.2.2 Discrete-time state space model

Equation (2) and (8) can be converted to discrete-time domain through zero-order hold assumption:

$$\mathbf{x}_{[k+1]} = \mathbf{A}_d \mathbf{x}_{[k]} + \mathbf{B}_d \ddot{\mathbf{u}}_{g[k]} \quad (9)$$

$$\mathbf{y}_{[k]} = \mathbf{C}_d \mathbf{x}_{[k]} \quad (10)$$

$\mathbf{x}_{[k]} = \mathbf{x}(k\Delta t)$ ,  $\mathbf{y}_{[k]} = \mathbf{y}(k\Delta t)$ , and  $\ddot{\mathbf{u}}_{g[k]} = \ddot{\mathbf{u}}_g(k\Delta t)$ , with  $k = 1, 2, \dots, n_t$ ,  $\Delta t$  the sample time, and  $n_t$  the total number of sampled points. The discrete-time system matrices  $\mathbf{A}_d$ ,  $\mathbf{B}_d$ , and  $\mathbf{C}_d$  are given by:

$$\mathbf{A}_d = \exp(\mathbf{A}_c \Delta t), \mathbf{B}_d = \mathbf{A}_c^{-1} (\mathbf{A}_d - \mathbf{I}_{n_s}) \mathbf{B}_c, \mathbf{C}_d = \mathbf{C}_c \quad (11)$$

where  $\mathbf{I}_{n_s} \in \mathbb{R}^{n_s \times n_s}$  is identity matrix.

## 2.3 Proposed strategy

In the presence of noise, modeling error, and incomplete absolute acceleration measurements, input and state estimation for earthquake-excited building structures is still challenging due to the absence of direct feedthrough, which leads to weak observability of the system input. In this thesis, a two-step strategy is proposed which consists of the least-squares algorithm and Kalman filtering to estimate input and state for building structures utilizing a limited number of absolute acceleration measurements.

### 2.3.1 Input Reconstruction

The proposed strategy estimates the ground input in the first step using an offline strategy. By substituting Equation (9) into Eq. (10) with zero initial conditions, the measurement equation  $\mathbf{y}_{[k]}$  can be rewritten as a matrix form [21]:

$$\mathbf{Y} = \mathbf{H}\ddot{\mathbf{U}}_g \quad (12)$$

$\mathbf{Y} \in \mathbb{R}^{n_d n_t}$  is the collected absolute acceleration response vector,  $\ddot{\mathbf{U}}_g \in \mathbb{R}^{n_t}$  is the collected ground input vector, and  $\mathbf{H} \in \mathbb{R}^{n_d n_t \times n_t}$  is the lower-block triangular Hankel matrix which contains the system Markov parameters, given by

$$\mathbf{Y} = \{\mathbf{y}_{[1]} \quad \mathbf{y}_{[2]} \quad \dots \quad \mathbf{y}_{[n_t]}\}^T \quad (13)$$

$$\mathbf{H} = \begin{bmatrix} \mathbf{C}_d \mathbf{B}_d & \mathbf{0} & \dots & \mathbf{0} \\ \mathbf{C}_d \mathbf{A}_d \mathbf{B}_d & \mathbf{C}_d \mathbf{B}_d & \dots & \mathbf{0} \\ \vdots & \vdots & \ddots & \mathbf{0} \\ \mathbf{C}_d \mathbf{A}_d^{n_t-1} \mathbf{B}_d & \mathbf{C}_d \mathbf{A}_d^{n_t-2} \mathbf{B}_d & \dots & \mathbf{C}_d \mathbf{B}_d \end{bmatrix} \quad (14)$$

$$\ddot{\mathbf{U}}_g = \{\ddot{\mathbf{u}}_{g[0]} \quad \ddot{\mathbf{u}}_{g[1]} \quad \dots \quad \ddot{\mathbf{u}}_{g[n_{t-1}]}\}^T \quad (15)$$

From Equation (12), the unknown ground input vector  $\ddot{\mathbf{U}}_g$  can be solved using ordinary least squares by minimizing the residual:

$$\mathbf{J}(\ddot{\mathbf{U}}_g) = \|\mathbf{H}\ddot{\mathbf{U}}_g - \mathbf{Y}\|^2 \quad (16)$$

However, the ordinary least squared solution of Equation (16) may yield unreliable results and unbounded errors due to rank deficiency of the observability matrix and weak observability of system. Therefore, the Tikhonov regularization method and Bayesian inference can be used to give a reliable result [22-25], namely,

$$\mathbf{J}(\ddot{\mathbf{U}}_g) = \|\mathbf{H}\ddot{\mathbf{U}}_g - \mathbf{Y}\|^2 + \lambda \|\ddot{\mathbf{U}}_g\|^2 \quad (17)$$

where  $\lambda$  is a symmetric positive definite matrix. The resulting solution of Equation (17) is given by

$$\hat{\ddot{\mathbf{U}}}_g = (\mathbf{H}^T \mathbf{H} + \lambda)^{-1} \mathbf{H}^T \mathbf{Y} \quad (18)$$

### 2.3.2 State Estimation

With the reconstructed ground input, the state vector, which consists of the relative displacement and velocity, can be estimated using the classical Kalman filter [27]. In order to consider the process noise and measurement noise,  $\mathbf{w}_{[k]}$  and  $\mathbf{v}_{[k]}$  are added to Equation (9) and (10), respectively. The vectors  $\mathbf{w}_{[k]}$  and  $\mathbf{v}_{[k]}$  are assumed to be zero-mean Gaussian white noise with known covariance matrices  $\mathbf{R} = \mathbb{E}[\mathbf{v}_{[k]} \mathbf{v}_{[l]}^T] > 0$  and  $\mathbf{Q} = \mathbb{E}[\mathbf{w}_{[k]} \mathbf{w}_{[l]}^T] \geq 0$ , and mutually uncorrelated.

After applying the initial state  $\hat{\mathbf{x}}_{[0|-1]}$  and the initial error covariance  $\mathbf{P}_{[0|-1]}$ , the state vector  $\hat{\mathbf{x}}_{[k|k]}$  is identified in two steps, including measurement update and time update, using a limited number of absolute acceleration measurement vector  $\mathbf{y}_{[k]}$  and the reconstructed ground input vector  $\hat{\mathbf{u}}_{g[k]}$  obtained from the least squares algorithm. The state estimation is given by the following equations [28, 29]:

Measurement update:

$$\mathbf{K}_{[k]} = \mathbf{P}_{[k|k-1]} \mathbf{C}^T / (\mathbf{C} \mathbf{P}_{[k|k-1]} \mathbf{C}^T + \mathbf{R}) \quad (19)$$

$$\hat{\mathbf{x}}_{[k|k]} = \hat{\mathbf{x}}_{[k|k-1]} + \mathbf{K}_{[k]} (\mathbf{y}_{[k]} - \mathbf{C} \hat{\mathbf{x}}_{[k|k-1]}) \quad (20)$$

$$\mathbf{P}_{[k|k]} = (\mathbf{I} - \mathbf{K}_{[k]} \mathbf{C}) \mathbf{P}_{[k|k-1]} \quad (21)$$

$$\hat{\mathbf{y}}_{[k|k]} = \mathbf{C} \hat{\mathbf{x}}_{[k|k]} \quad (22)$$

Time update:

$$\hat{\mathbf{x}}_{[k+1|k]} = \mathbf{A} \hat{\mathbf{x}}_{[k|k]} + \mathbf{B} \hat{\mathbf{u}}_{g[k]} \quad (23)$$

$$\mathbf{P}_{[k+1|k]} = \mathbf{A} \mathbf{P}_{[k|k]} \mathbf{A}^T + \mathbf{Q} \quad (24)$$

$\hat{\mathbf{y}}_{[k]}$  is the estimated response vector at unmeasured locations. A large value for the initial error covariance  $\mathbf{P}_{[0|-1]}$  is recommended.

## 2.4 The proposed strategy for joint input-state estimation for earthquake-excited building structures

As illustrated in Figure 2.1, after constructing  $\mathbf{H}$  from the system matrices  $\mathbf{A}_d$ ,  $\mathbf{B}_d$ , and  $\mathbf{C}_d$ , and assembling absolute acceleration measurements in  $\mathbf{Y}$ , the least-squares algorithm with Tikhonov regularization defined in Section 2.3.1 is applied to identify the ground input using only absolute acceleration measurements. Then, the states are estimated with the Kalman filter utilizing the estimated ground input and measured absolute floor acceleration responses.

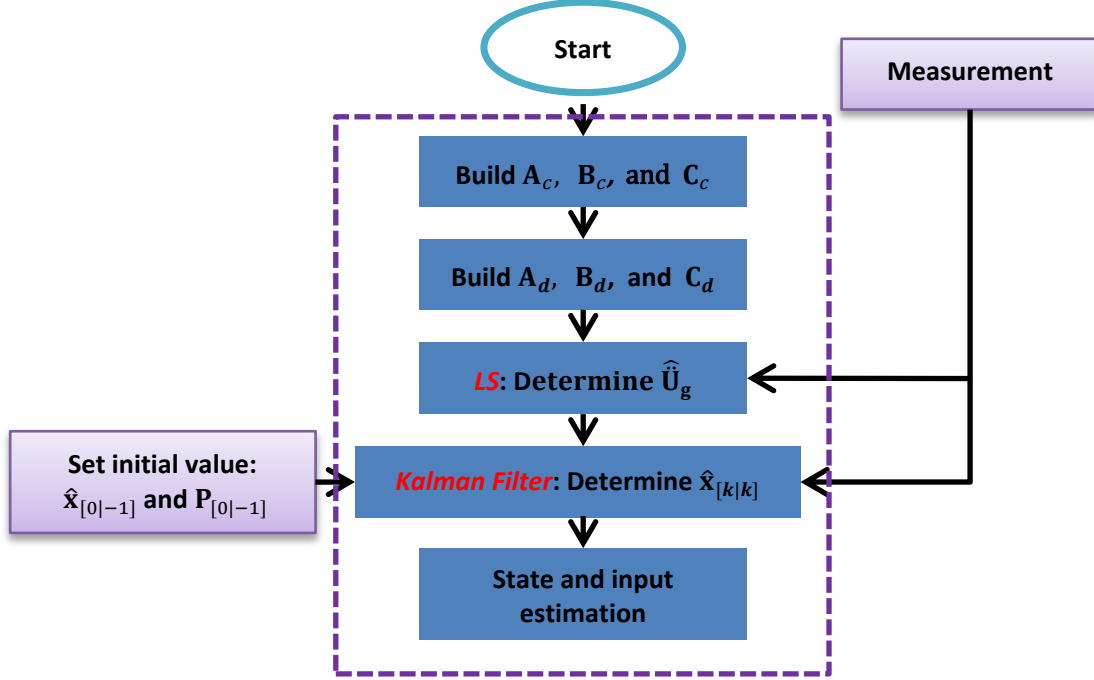


Figure 2.1: Flowchart of the proposed two-step strategy

## 2.5 Online state and input estimation

In this section, the online method for unbiased minimum-variance input and state estimation proposed in [13, 14], termed the Gillijns Algorithm, is presented. The method consists of three steps: time update, estimation of unknown input, and measurement update. The unknown ground input  $\hat{\mathbf{u}}_{g[k]}$  is determined using the following equation:

$$\hat{\mathbf{x}}^*_{[k|k-1]} = \mathbf{A} \hat{\mathbf{x}}^*_{[k-1|k-1]} \quad (25)$$

$$\hat{\mathbf{u}}_{g[k-1]} = \mathbf{M}_{[k]}(\mathbf{y}_{[k]} - \mathbf{C} \hat{\mathbf{x}}^*_{[k|k-1]}) \quad (26)$$

$\mathbf{M}_{[k]}$  is input gain which is updated at each time  $k$  using the error covariance matrix  $\mathbf{P}^*_{[k|k-1]}$ .

$\hat{\mathbf{x}}^*_{[k|k-1]}$  is the biased state vector. The  $\mathbf{P}^*_{[k|k]}$  is given by:

$$\mathbf{P}^*_{[k|k-1]} = \mathbb{E}[(\mathbf{x}_{[k]} - \hat{\mathbf{x}}^*_{[k|k-1]})(\mathbf{x}_{[k]} - \hat{\mathbf{x}}^*_{[k|k-1]})^T] \quad (27)$$



From Equation (26), the unknown  $\hat{\mathbf{u}}_{g[k-1]}$  is estimated with one time step delay since measurement  $\mathbf{y}_{[k]}$  at first step  $k$  doesn't have information about input. It is noted that the unbiasedness of the  $\hat{\mathbf{u}}_{g[k-1]}$  was obtained through the criterion  $\mathbf{M}_{[k]}\mathbf{CB}=\mathbf{I}$ .

## 2.6 Observability of system input

The observability matrix of system input is described here. To determine the observability of the system input and the stability of the algorithms, rank and condition of the observability matrix should be known. Thus, from Equation (12), the observability matrix can be written as:

$$\mathbf{O} = \begin{bmatrix} \mathbf{C}_d \mathbf{A}_d & \mathbf{C}_d \mathbf{B}_d & \mathbf{0} & \dots & \mathbf{0} \\ \mathbf{C}_d \mathbf{A}_d^2 & \mathbf{C}_d \mathbf{A}_d \mathbf{B}_d & \mathbf{C}_d \mathbf{B}_d & \dots & \mathbf{0} \\ \vdots & \vdots & \vdots & \ddots & \mathbf{0} \\ \mathbf{C}_d \mathbf{A}_d^L & \mathbf{C}_d \mathbf{A}_d^{L-1} \mathbf{B}_d & \mathbf{C}_d \mathbf{A}_d^{L-2} \mathbf{B}_d & \dots & \mathbf{C}_d \mathbf{B}_d \end{bmatrix} \quad (28)$$

Where  $\mathbf{O} \in \mathbb{R}^{n_d L \times (L+(n_s))}$  is the observability of the system input and  $L$  is the number of sampled points. To ensure the system input is observable, the matrix  $\mathbf{O}$  has to have a full column rank and be well-conditioned.

## 2.7 Summary

In this chapter, the mathematical formulation of the proposed strategy was presented for systems without direct feedthrough to estimate state and input, with a particular focus on earthquake-excited building structures. The proposed strategy contains two steps: First, the input is reconstructed by solving a least squares problem with Tikhonov regularization and Bayesian inference. Second, the Kalman filter with input term obtained from the first step is applied to identify states and responses at unmeasured locations. An online joint state-input estimation method, termed the Gillijns Algorithm, was also described for comparison purpose. It is noted that both strategies, the offline and online, depend on the least squares method to estimate input.

The algorithms presented in this chapter will be applied in chapter 3 and chapter 4 to examine their robustness and effectiveness.

## **Chapter 3 : NUMERICAL INVESTIGATION**

In this chapter, the proposed strategy presented in Chapter 3 is numerically examined using a four-story shear-type building structure to verify its effectiveness and robustness. At the start of the chapter, the numerical model is described. Next, the performance of the proposed strategy on the numerical model is evaluated using two different types of inputs, including a stationary and a non-stationary ground input. In the presence of various levels of noise, modelling errors, and partial measurements, the results of the numerical simulation obtained from the proposed strategy are discussed, and are further compared with the online method presented in Chapter 3. At the end of the chapter, the results are summarized.

This chapter is organized as follows: Section 3.1 defines the numerical model; Section 3.2 and Section 3.3 discuss the results of the numerical model under a stationary and non-stationary ground input using the proposed strategy; Section 3.4 assesses the results obtained from the proposed strategy by comparing it with an online algorithm; Section 3.5 summarizes this chapter.

### **3.1 Numerical model**

To investigate the accuracy and robustness of the proposed strategy, as shown in Figure 3.1, a numerical model of a four-story shear-type building structure is adopted. The floor mass and stiffness values are listed in Table 3.1. All four modal damping ratios are defined as 4%. Table 3.2 shows two cases with four and two acceleration measurements for investigating the effect of the number of measurements.

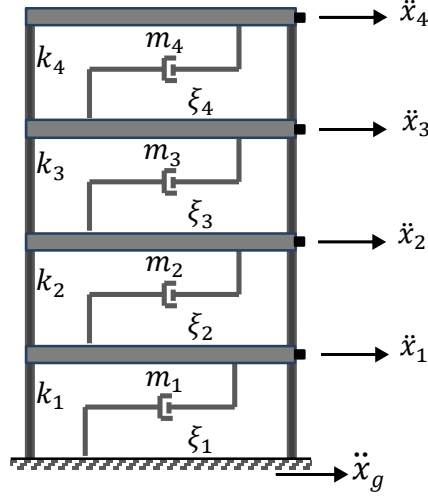


Figure 3.1: A four-story shear-type building

Table 3.1: Structural parameters

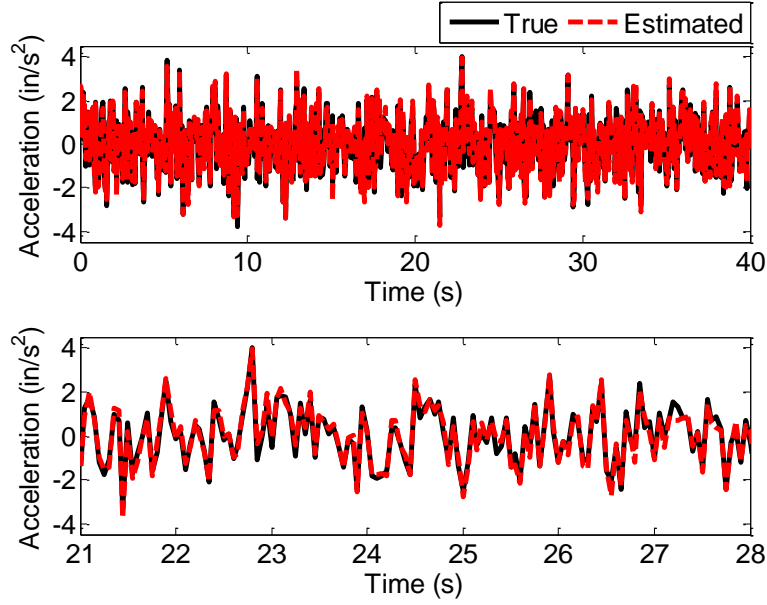
Floor number	1	2	3	4
Mass (Kip-sec <sup>2</sup> /in)	2	2	1.5	1.5
Stiffness (Kip/in)	3200	2400	1600	800

Table 3.2: Two cases with different sensing information

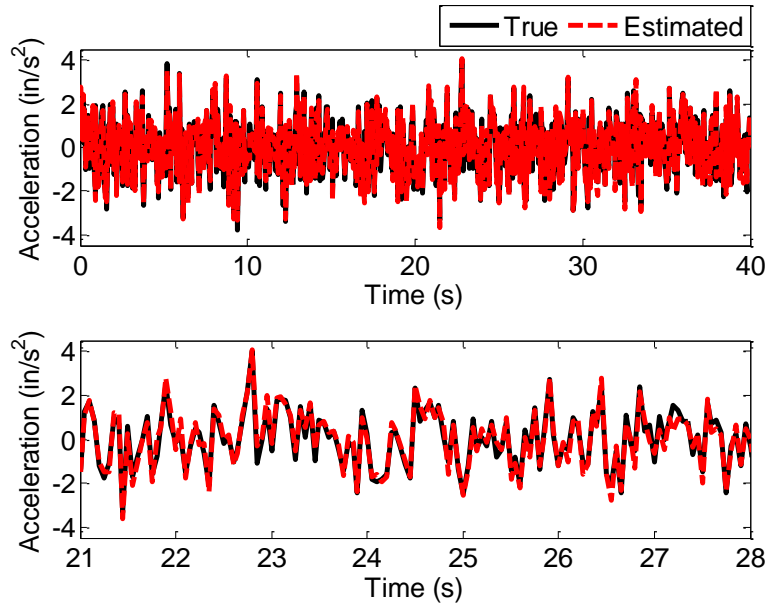
Case	No. of acceleration measurements	Location of measurement
1	4	1 <sup>st</sup> , 2 <sup>nd</sup> , 3 <sup>rd</sup> , 4 <sup>th</sup> , floors
2	2	2 <sup>nd</sup> , and 4 <sup>th</sup> floors

To consider the effect of modelling error and measurement noise on the proposed strategy, modeling errors are introduced by increasing the stiffness and damping ratio by a certain percentage, e.g. 2%, and various levels of measurement noise are considered by adding a zero-mean Gaussian white noise to the simulated absolute floor accelerations. To quantify the

accuracy of the results, the frequency domain error (FDE) [30] is adopted to account for both the amplitude and phase errors. Finally, to illustrate the robustness, the ground input estimated from the proposed strategy is compared with the online methodology presented in Section 2.5.



(a) Case 1: amplitude error = 6.5%, phase error = 3.2%, FDE = 9.7%



(b) Case 2: amplitude error = 7.6%, phase error = 4%, FDE = 11.6%

Figure 3.2: Ground input estimation with 12% measurement noise and 5% modeling error

Two types of input loading, including stationary and non-stationary ground inputs, are investigated. By following the procedure described in Figure 2.1, the proposed strategy is applied for input estimation based on the measurement and model, the measurement  $\mathbf{y}_{[k]}$ , and the  $\mathbf{A}_d$ ,  $\mathbf{B}_d$ , and  $\mathbf{C}_d$  matrices. The measurement vector  $\mathbf{y}_{[k]}$  contains the absolute acceleration responses, for which two measurement cases are considered as shown in Table 3.2. The matrices  $\mathbf{A}_d$ ,  $\mathbf{B}_d$ , and  $\mathbf{C}_d$  are constructed from the mass, stiffness values listed in Table 1 and the damping ratios. Next, the Kalman filter is applied combining the estimated ground input obtained from step 1 to identify floor states. Here, the initial state vector  $\hat{\mathbf{x}}_{[0|-1]}$  for the Kalman filter is set to zero. The matrices  $\mathbf{Q}$ ,  $\mathbf{R}$ , and  $\mathbf{P}_{[0|-1]}$  are set to be  $10^{-1}$ ,  $10^{-1}$  and  $10^3$  on the diagonal, respectively.

### 3.2 Stationary ground input

In this section, the performance of the proposed strategy is assessed under a stationary ground input (Band Limited White Noise) by considering different measurement noise, number of measurements and modelling error. The sampling rate and input duration are 20 Hz and 40 sec, respectively.

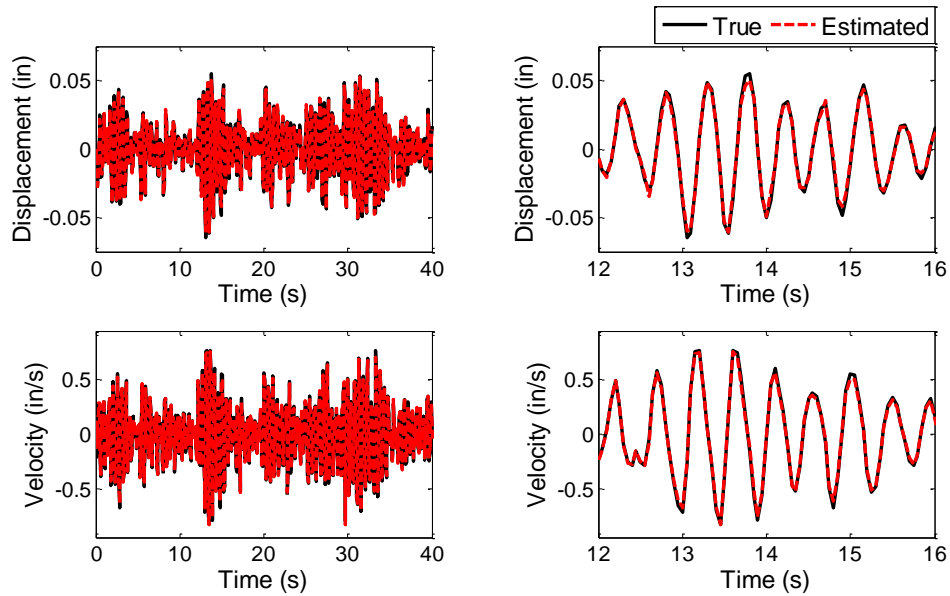
#### 3.2.1 Input estimation results

The reconstructed input ground motions for Case 1 (four floor accelerations) and Case 2 (two floor accelerations) are shown in Figure 3.2. A 12% measurement noise and a 5% modeling error are considered in both cases. Overall, the estimated ground inputs agree well with the corresponding actual ground inputs. Satisfactory FDEs, 9.7% and 11.6% for Case 1 and Case 2, are seen from the figure. In Case 2 when less sensing information is used, a slightly larger FDE is obtained in the result. However, considering the level of modeling error and measurement

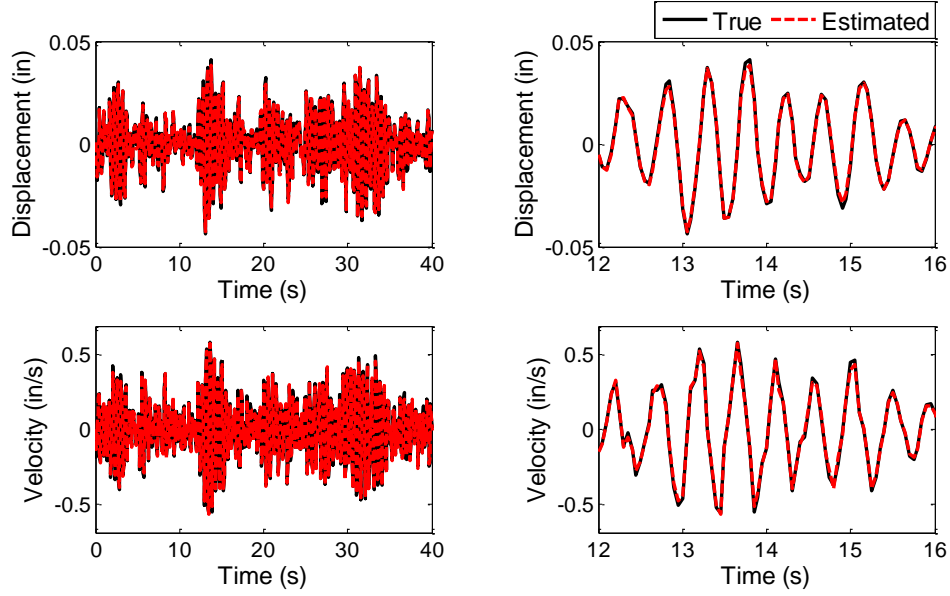
noise considered in the analyses, and the proposed input estimation strategy show satisfactory performance in both cases.

### 3.2.2 State estimation results

Figure 3.3 shows the state estimation results using Kalman filter based on the input estimated from Section 3.2.1. Specifically, Figure 3.3(a) shows the estimated displacement and velocities at the 4<sup>th</sup> floor, while Figure 3.3(b) illustrates the results for Case 2 at the 3<sup>rd</sup> floor, where no sensing information is used in state estimation. The associated FDEs are also shown in each figure. Overall, the estimated states agree very well with the true states, with 12.9% and 6.3% FDEs for Case 1 and Case 2, respectively. In addition, it is noted that incomplete floor acceleration measurements do not seem to have negative effect on state estimation. The result demonstrates the robustness of the proposed strategy in state estimation in the presence of limited measurements, measurement noise, and modelling error.



(a) Case 1: state estimation at the 4<sup>th</sup> floor  
Amplitude error = 9.4%, phase error = 3.4%, FDE = 12.9%



(b) Case 2: state estimation at the 3<sup>rd</sup> floor  
Amplitude error = 4.3%, phase error = 2%, FDE = 6.3%

Figure 3.3: State (relative displacement and velocity) estimation with 12% measurement noise and 5% modeling error

In addition to state estimation, in Case 2, absolute floor acceleration responses are estimated at unmeasured locations. Figure 3.4 shows the comparison between the true and the estimated absolute acceleration at the 3<sup>rd</sup> floor. The estimated response shows a good agreement with the true response. Moreover, an acceptable FDE, 14.1%, is observed from the figure. Hence, the proposed strategy achieved good performance in estimation of both states and responses at unmeasured locations.



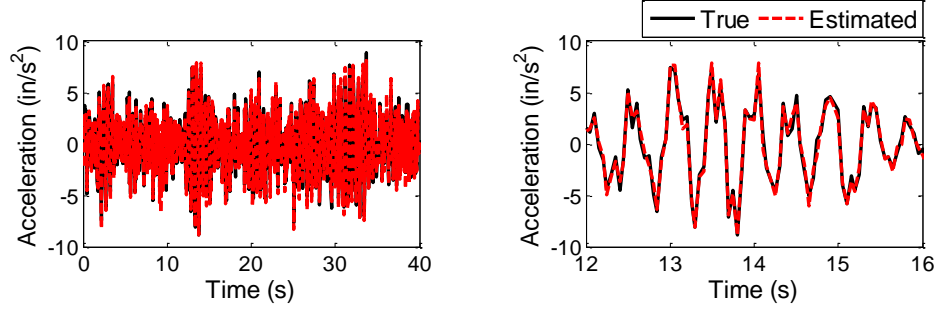


Figure 3.4: Estimated absolute acceleration at the unmeasured (3rd) floor in case 2, with 12% measurement noise and 5% modeling error. (Amplitude error = 9%, phase error = 5.1%, FDE = 14.1%)

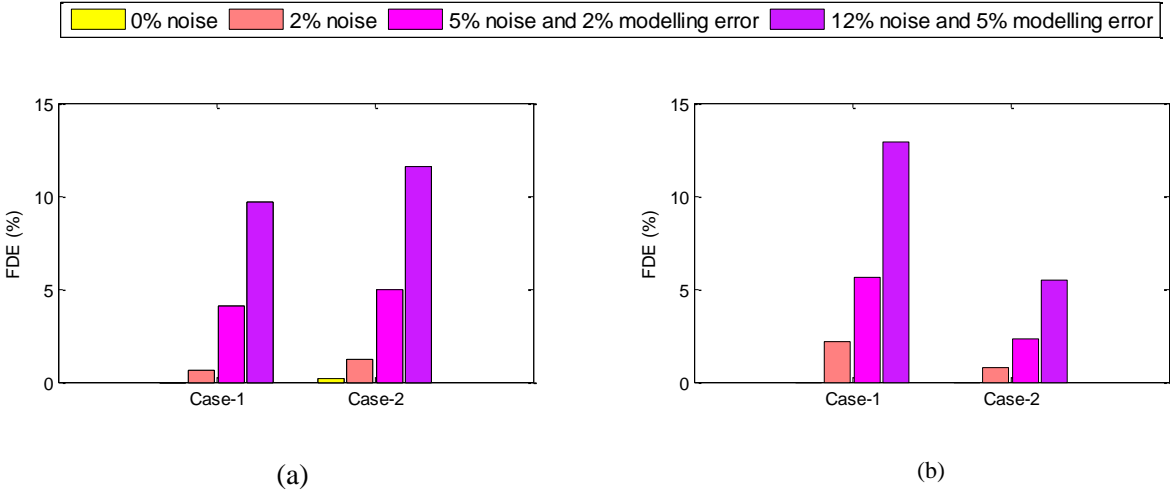


Figure 3.5: The frequency domain errors (FDE) of (a) input estimation, and (b) displacement estimation at the 4th floor under different levels of measurement noise and modeling error

### 3.2.3 Input-state estimation under different level of measurement noise and modeling errors

In this section, the levels of measurement noise and modeling error for both Case 1 and Case 2 are varied, and the associated FDEs for input and state estimations are shown in Figure 3.5. First of all, when no measurement noise is present, full acceleration measurement (Case 1) achieved near perfect input and state estimations. However, when only partial floor acceleration measurements are available (Case 2), the estimated input shows a slightly higher error. On the other hand, the accuracies of state estimations are equally good between these two cases,

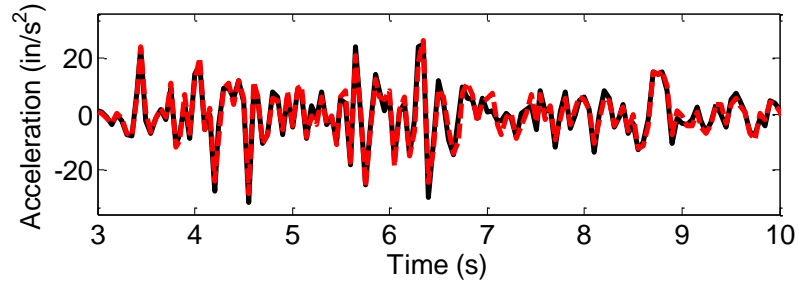
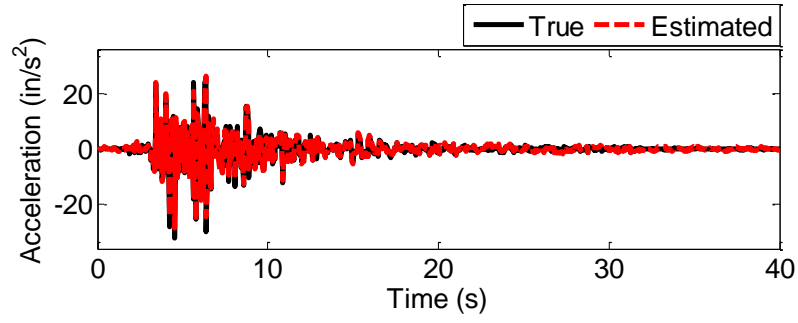
indicating incomplete measurement has higher impact on input estimation compared with state estimation. In fact, as shown in Figure 3.3(b), the accuracy of state estimation is consistently higher in Case 2 when partial floor accelerations are used. This could be attributed to the fact that less noise is introduced by using a smaller number of noisy measurements.

### **3.3 Joint state-input estimation based on a non-stationary earthquake input**

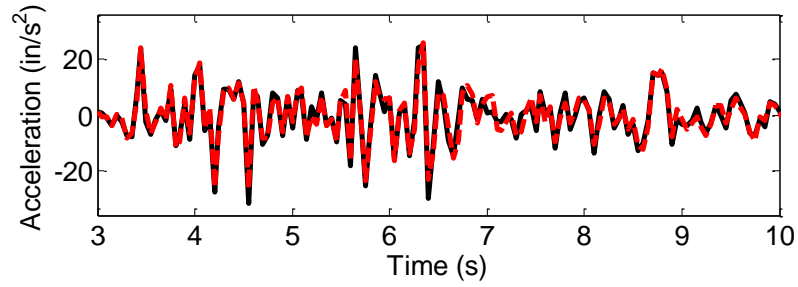
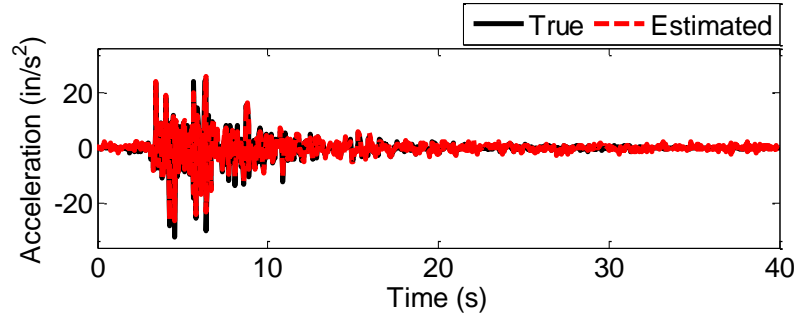
In this section, a non-stationary earthquake ground input is applied for state and input estimation considering measurement noise, modelling error, and incomplete measurement. Similar to the case of the stationary ground input, the sampling rate and duration are 20 Hz and 40 sec, respectively. The Peak Ground Acceleration (PGA) of the ground input is  $25 \text{ in/s}^2$ .

#### **3.3.1 Input estimation results**

The results of the proposed strategy for the reconstructed non-stationary ground input are discussed here. Figure 3.6 depicts the estimated non-stationary ground input under 12% measurement noise and 5% modelling error for Case 1 and Case 2. The estimated non-stationary ground inputs show a satisfactory agreement with the corresponding ground inputs for both cases. By comparing the stationary and non-stationary ground input cases, the FDEs seen from both cases are close to each other, indicating the effectiveness and robustness of the proposed strategy in estimating non-stationary inputs.



(a) Case 1: amplitude error = 7.3 %, phase error = 3.9%  
FDE = 11.1%

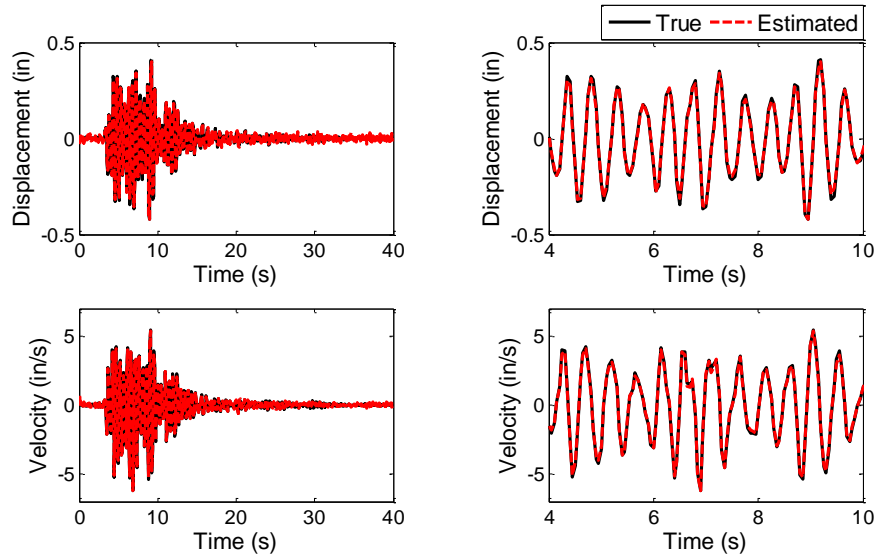


(b) Case 2: amplitude error = 9.5%, phase error = 5%  
FDE = 14.5%

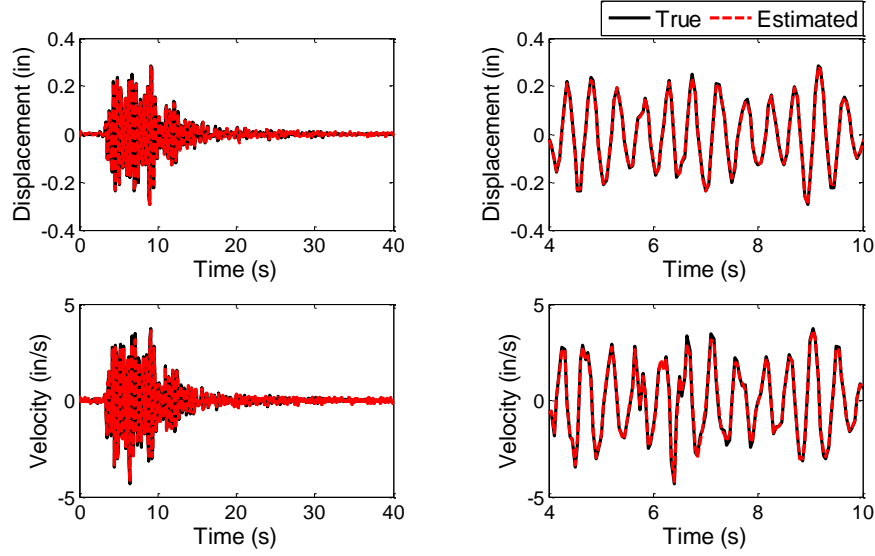
Figure 3.6: Non-stationary ground input estimation with 12% measurement noise and 5% modeling error

### 3.3.2 State estimation results

Figure 3.7(a) and Figure 3.7(b) show the estimated states under 12% measurement noise and 5% modelling error at the 4<sup>th</sup> and 3<sup>rd</sup> floors for Case 1 and Case 2, respectively. Similar to the case of stationary ground input, the estimated states are very close to the true ones, yielding satisfactory FDEs. Similarly, Figure 3.8 compares the identified absolute acceleration at floor 3<sup>rd</sup> for Case 2 with the corresponding true acceleration. A good agreement is seen between the estimated and the true responses. Overall, the proposed strategy for state and response estimation under non-stationary input is shown effective, with similar level of FDEs observed from the stationary input case.



(a) Case 1: state estimation at the 4<sup>th</sup> floor  
Amplitude error = 12%, phase error = 3.1%, FDE = 15.1%



(b) Case 2: state estimation at the 3<sup>rd</sup> floor  
Amplitude error = 5.4%, phase error = 2.2%, FDE = 7.6%

Figure 3.7: State (relative displacement and velocity) estimation with 12% measurement noise and 5% modeling error

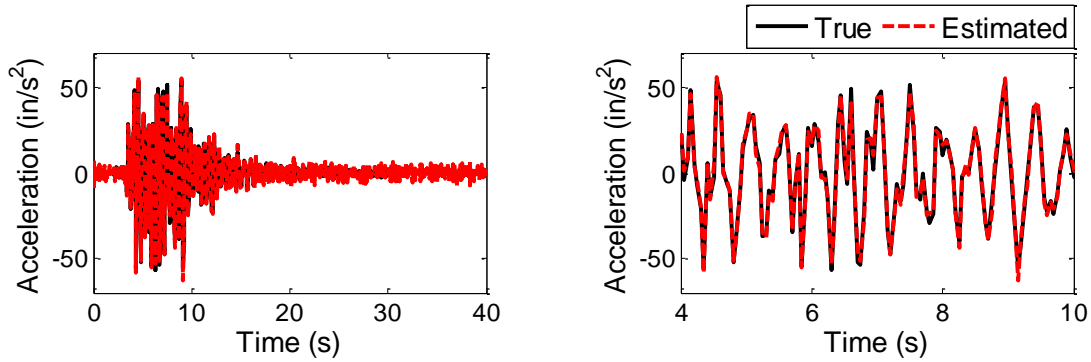


Figure 3.8: Estimated absolute acceleration at the unmeasured (3rd) floor in case 2, with 12% measurement noise and 5% modelling error. (Amplitude error = 11.2%, phase error = 6.1%. FDE = 17.3%)

### 3.4 Comparative study

In this section, the performance of the proposed strategy for input estimation is compared with the online method presented in Section 2.5, termed the Gillijns Algorithm. In this comparison, both Case 1 and Case 2 are considered with 12% measurement noise and 5% modelling error.

Figure 3.9(a) and Figure 3.9(b) demonstrate the comparison of input estimation between the Gillijns Algorithm and the proposed strategy. Due to the weak observability of the ground input, unstable results are obtained using the online estimation method in the presence of measurement noise and modeling error. On the other hand, the proposed offline strategy for input estimation achieved stable input estimation even using incomplete floor acceleration measurements.

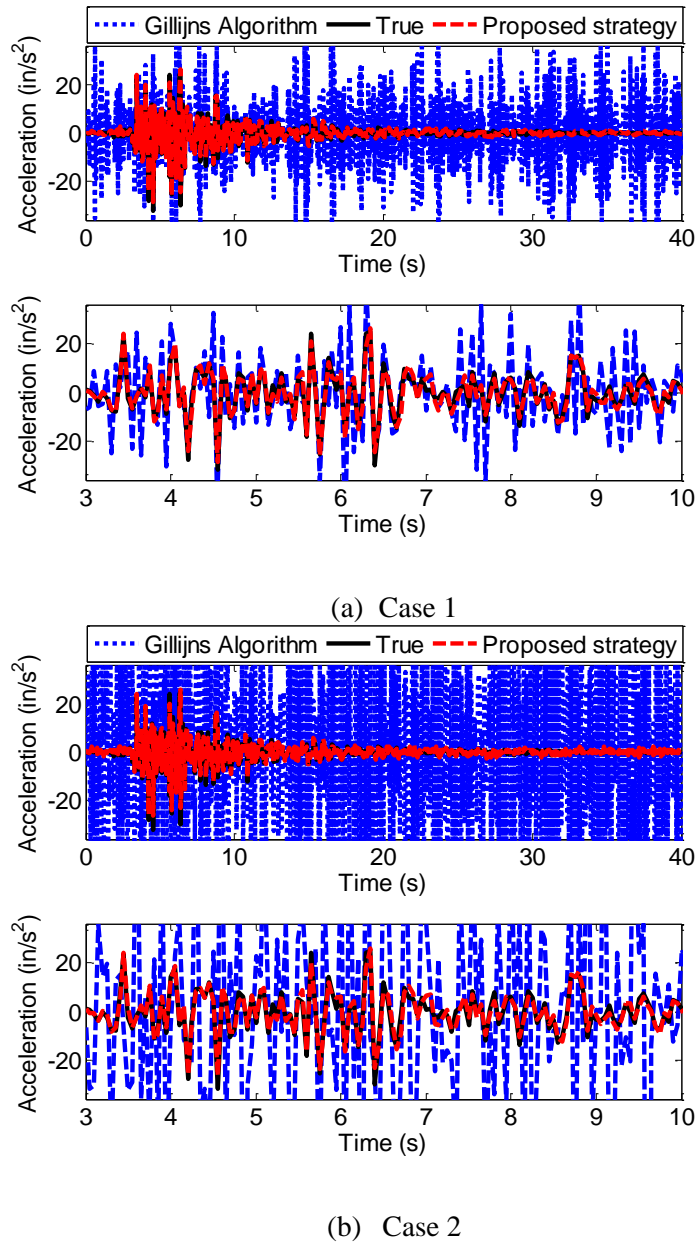


Figure 3.9: Non-stationary ground input estimations with 12% measurement noise and 5% modeling error

### 3.5 Summary

This chapter presented the performance of the proposed strategy in estimating ground input and state for earthquake-excited building structures utilizing absolute acceleration measurements. A numerical example for a four-story shear-type building structure under stationary and non-stationary ground input was performed to confirm the robustness of the proposed strategy. The accuracy of the proposed strategy indicated using the frequency domain error (FDE), which accounts for the amplitude and phase errors. Overall, the results of the numerical example confirmed the effectiveness and robustness of the proposed strategy in estimating states, responses at unmeasured locations, and ground input in the presence of noise, modeling error, and partial measurements.

## **Chapter 4 : EXPERIMENTAL INVESTIGATION**

In this chapter, applicability and robustness of the proposed strategy is further confirmed through a laboratory experiment. The laboratory model, which consists of a scaled six-story frame structure, is introduced at the beginning of the chapter, for which absolute accelerations at each floor and the reference displacement at top floor are measured using accelerometers and a smartphone camera. Then, the proposed strategy is applied to estimate input, state, and response utilizing a limited number of the measured absolute accelerations. Finally, experimental results are discussed, demonstrating the effectiveness of the proposed strategy.

This chapter is organized as follows: Section 4.1 introduces laboratory model and measurement setup that will be used for the experimental investigation; Section 4.2 discusses the experimental model and measurements; Section 4.3 illustrates the results obtained from proposed strategy using the experimental model and measurements defined in Section 4.2; Summary of the chapter is discussed in Section 4.4.

### **4.1 Laboratory model and measurement setup**

The performance of the proposed strategy is examined on a scaled six-story laboratory frame structure using shake table tests at University of Kansas (Figure 4.1). The laboratory experiment conducted by [33] is used in this chapter. For the sake of completeness, details of the experimental testing are presented in this section. The laboratory model installed on the shake table consists of the steel columns ( $12 \times 1.25 \times 0.125$  in) and the floor plates ( $18 \times 12 \times 0.375$  in), which are connected together using bolts and angles. The mass of first, second, third, fourth, and fifth floors are  $1.16 \times 10^{-4}$  Kip.sec<sup>2</sup>/in, while the sixth floor is  $1.10 \times 10^{-4}$  Kip.sec<sup>2</sup>/in. The structure is excited by the hydraulic shaker at the base.



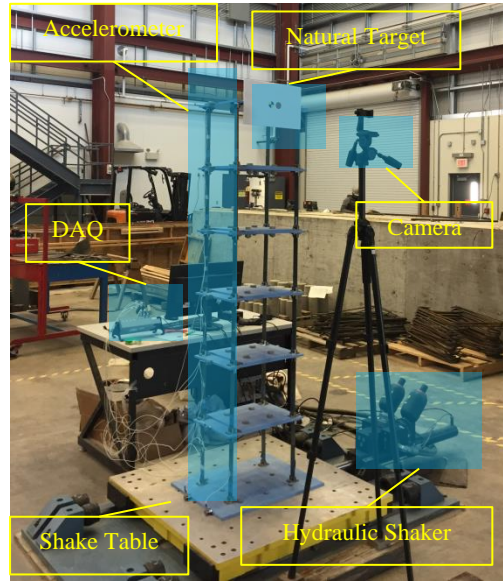


Figure 4.1: The six-story laboratory frame structure and measurement setup

Seven accelerometers (PCB 353B33 with sensitivity around 102.8 mV/g), LVDT installed with the shake table, and a smartphone camera were used to measure the accelerations, ground displacement, and absolute displacement responses, respectively. The overview of the accelerometer and the smartphone locations are indicated in Figure 4.1. The accelerometers were attached to each floor utilizing a magnet to measure absolute acceleration responses. An accelerometer was also installed on top of the shake table to measure the ground input (ground acceleration) as a reference. In addition, a smartphone camera (iPhone 6) mounted on a tripod was positioned next to the shake table and the structure. For comparison purpose, the RINO app for real time displacement measurement developed by Min et al. [31] with the smartphone camera was used to record absolute displacement at top floor using a colored target during testing.

The acceleration data obtained from the accelerometers was collected at a sampling frequency of 2048 Hz using the National Instruments (NI) DAQ system. For LVDT and the

smartphone, a sampling frequency of 125 Hz and a frame rate of 120 fps with spatial resolution of 720p were employed, respectively. The absolute displacement obtained from the smartphone was synchronized with the ground displacement data measured by the shake table LVDT. Next, the ground displacement was subtracted from the absolute displacement obtained from the smartphone in order to obtain the reference relative displacement measurement, which is denoted as the measured relative displacement. Moreover, all measurements were resampled to 28 Hz, which is larger than twice the maximum natural frequency of the building structure to ensure the contribution of the all six modes in the measured responses.

#### **4.2 Proposed strategy and system identification based on experimental study**

This chapter aims to apply the proposed strategy to experimentally identify ground input, state (displacement and velocity), and acceleration responses at unmeasured locations, based on limited acceleration measurements  $\mathbf{y}_{[k]}$  and the structural state space model, i.e.,  $\mathbf{A}_d$ ,  $\mathbf{B}_d$ , and  $\mathbf{C}_d$  matrices. For the measurements  $\mathbf{y}_{[k]}$ , only three absolute acceleration measurements obtained from the accelerometers at the 3<sup>rd</sup>, 5<sup>th</sup>, and 6<sup>th</sup> floors are used in the estimation. The model  $\mathbf{A}_d$ ,  $\mathbf{B}_d$ , and  $\mathbf{C}_d$  matrices are constructed through system identification. For input estimation, the model obtained from Eigensystem Realization Algorithm (ERA) [32] is directly employed. This is due to the fact that the ERA model is more accurate in describing the input-output relationship, although it lacks the physical meaning of the states. For state estimation, the dynamic model constructed based on the updated parameters obtained from experimentally identified natural frequencies and damping ratios listed in Table 4.1 are used. The reason is that the physical model based on calibrated structural parameters is necessary for Kalman filtering since it maintains the physical meanings of the states.

After analyzing the data and constructing the matrices  $\mathbf{A}_d$ ,  $\mathbf{B}_d$ , and  $\mathbf{C}_d$ , similar to the numerical example in Chapter 3, the suggested strategy follows the procedure described in Figure 2.1, applied to estimate the ground input using Equation 16, ordinary least square algorithm. In second step, floor states and unmeasured responses are estimated using Kalman filter with ground input obtained from the first step, based on the updated parameter-based model. Here, the matrices  $\mathbf{Q}$ ,  $\mathbf{R}$ , and  $\mathbf{P}_{[0|-1]}$  are assumed be  $10^3$ ,  $10^2$  and  $10^3$  on the diagonal, respectively, and the initial state vector  $\hat{\mathbf{x}}_{[0|-1]}$  assumed to be zero.

Table 4.1: Experimental natural frequencies and damping ratios for the six-story laboratory structure

No. of floor (mode)	1	2	3	4	5	6
Damping ratio (%)	0.8	0.6	0.8	0.3	0.4	0.21
Natural Frequency (Hz)	1.5	4.6	7.7	10	11.8	13

### 4.3 Joint input-state estimation based on earthquake input

The performance of the proposed strategy under a non-stationary earthquake input and partial measurements is experimentally studied here. One of the non-stationary ground inputs recorded during the Northridge earthquake of January, 1994 was used to run the test using the shake table. The non-stationary ground input was the recorded ground motion at the Burbank 6-story commercial building (CGS station 24370, Channel 9). The procedures defined in Section 4.1 and Section 4.2 were applied to collect data and construct the model. After analyzing the data and constructing the model, the proposed strategy was applied to estimate the ground input, state, and absolute acceleration responses at unmeasured location using only three absolute acceleration measurements obtained from the accelerometers at the 3<sup>rd</sup>, 5<sup>th</sup>, and 6<sup>th</sup> floors. The remaining measured accelerations at the 1<sup>st</sup>, 2<sup>nd</sup>, and 4<sup>th</sup> floors are used as a reference to compare with the

corresponding estimated absolute acceleration responses. Similarly, the estimated ground input and displacement from the proposed strategy are compared with the measured ground input obtained from the accelerometer installed on the shake table and the reference (measured) relative displacement obtained from the smartphone and the LVDT, respectively.

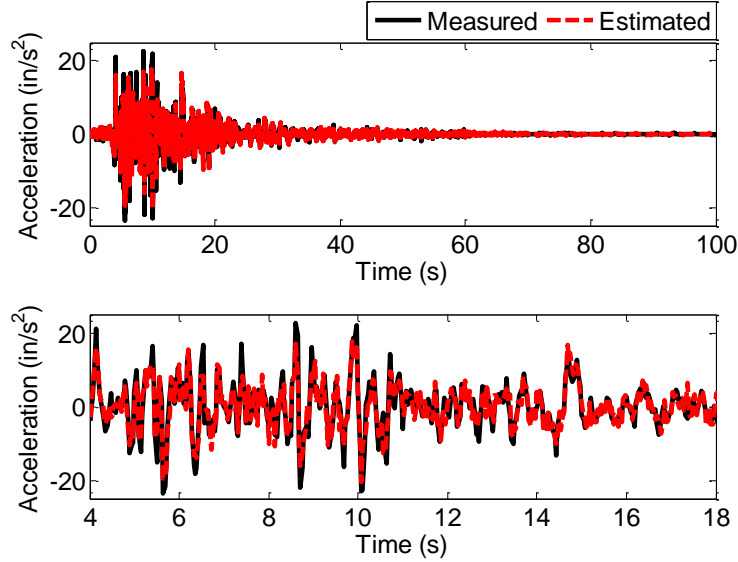


Figure 4.2: Time history of the ground input estimation (Top), and detail of the time history (bottom).  
(Amplitude error = 19.4 %, phase error = 9.1%, FDE = 28.5%)

#### 4.3.1 Ground input identification results

In this section, the experimental result for the estimated non-stationary ground input using the proposed strategy is described. Figure 4.2 shows the estimated ground input, the measured ground acceleration, and the associated FDE. The estimated ground input indicates an acceptable agreement with the measured one, yielding satisfactory FDE (28.5%). Some amplitude errors can be observed especially at peaks, which could be due to modelling error. Hence, similar to the numerical example, partial acceleration measurements under the experiment investigation achieved satisfactory performance, showing the proposed strategy is again robust and effective in input estimation.

#### 4.3.2 State estimation results

Using Kalman filter based on the proposed strategy, the relative displacements and velocities, and acceleration responses at unmeasured floors are estimated using only three absolute acceleration measurements at the 3<sup>rd</sup>, 5<sup>th</sup>, and 6<sup>th</sup> floors. Figure 4.3 compares the estimated relative displacement obtained from proposed strategy with the corresponding measured relative displacement at the 6<sup>th</sup> floor obtained from the smartphone camera and the LVDT. In the figure, the associated FDE is displayed as well. Overall, the estimated displacement agrees well with the measured displacement, showing acceptable FDEs (11.9%). From this experimental test, the proposed strategy demonstrates very good performance in estimation of displacement, further proving its applicability and effectiveness.

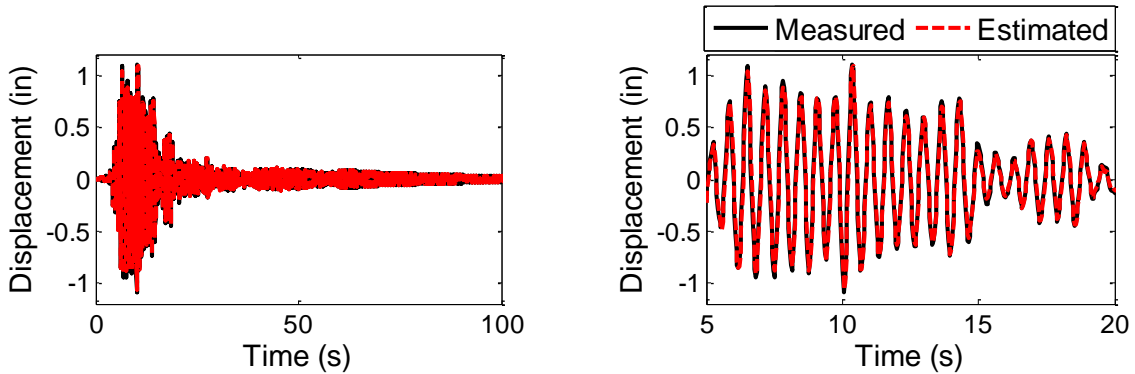


Figure 4.3: Time history of the estimated relative displacement at floor 6th (left), and detail of the time history (right). (Amplitude error = 3.9 %, phase error = 7.9 %, FDE = 11.9%)

Similar to floor displacements, the floor velocities are estimated. Due to the lack of velocity measurements in this research, the estimated velocities obtained from Kalman filter with the measured ground acceleration input are used as reference for the comparison. The result of the identified velocities obtained from Kalman filter with the estimated ground input and measured ground input are shown in Figure 4.4, indicating a very good agreement.

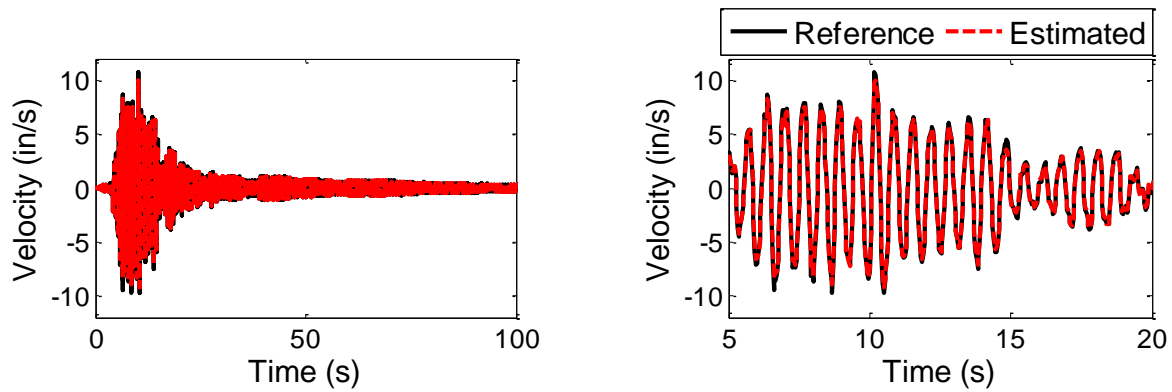


Figure 4.4: Time history of the estimated relative velocity at floor 6th (left), and detail of the time history (right)

Furthermore, responses at unmeasured floors are estimated. Figure 4.5 shows the estimated absolute acceleration response at the 4<sup>th</sup> floor, for which only measurements at the 3<sup>rd</sup>, 5<sup>th</sup>, and 6<sup>th</sup> floors were used. An acceptable result of the estimation is noted, with 15% amplitude error. However, there is still a discernable difference between the estimated and measured absolute acceleration responses. Again, this difference could be due to modelling error. Overall, good estimations for state and response were obtained using experimental data, demonstrating the applicability of the proposed strategy.

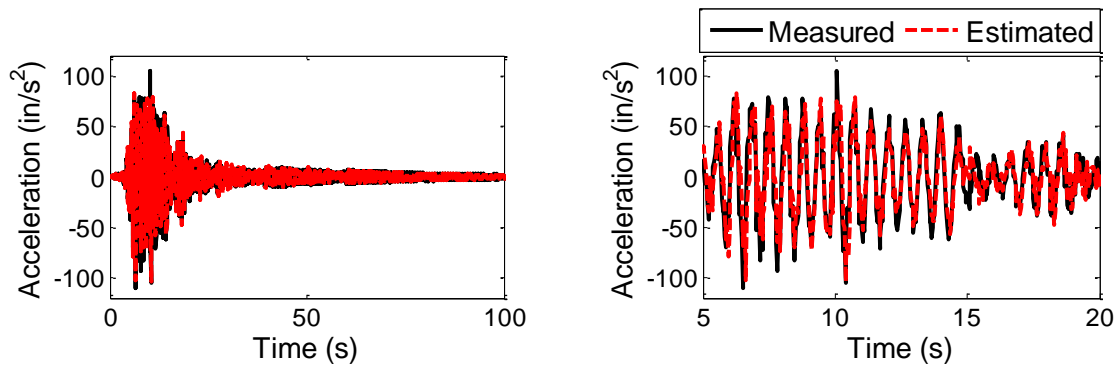


Figure 4.5: Time history of the absolute acceleration estimation at floor 4th (left), and detail of the time history (right). (Amplitude error = 15 %, phase error = 15.1 %, FDE = 30.1%)

#### **4.4 Summary**

In this chapter, the performance of the proposed strategy was experimentally examined based on a scaled six-story laboratory model. Experimental acceleration measurements were used in input and state estimation. The proposed strategy was applied to estimate input, state, and response using partial measurements. The estimated ground input and states based on the laboratory experiment showed good accuracy. Moreover, satisfactory results for response estimation at unmeasured locations were also obtained. Overall, the results from the laboratory experiment in this chapter showed good performance, indicating the effectiveness of the proposed strategy using real measurements.

## Chapter 5 : CONCLUSIONS

This chapter presents the conclusions and the main contributions of the thesis. Recommendations for future work are also discussed.

### 5.1 Conclusions and main contributions

This thesis investigated input and state estimation for earthquake-excited building structures using incomplete absolute acceleration response measurements. Utilizing responses in term of absolute accelerations renders the system without direct feedthrough. As a result, it leads to weak observability of the system input. The contribution of this research is the proposed strategy to estimate input and state for systems without direct feedthrough despite the issue of input observability.

The main contributions presented in this thesis are summarized as follows:

- In Chapter 2, in the context of input estimation, estimation of responses at unmeasured location, and state estimation, the mathematical formulation of the proposed two-step strategy was presented for systems without direct feedthrough, with a particular attention on earthquake-excited building structures. In the first step, input is estimated using an offline method by solving a least squares problem with Tikhonov regularization. In the second step, the Kalman filter in conjunction with the identified input from the first step is employed to estimate states and responses at unmeasured locations. In order to compare the proposed strategy with existing online methods, the online method for systems without direct feedthrough, the Gillijns Algorithm, was introduced. Moreover, the observability of system input was described to highlight the ill-conditioned problem.



- In Chapter 3, the performance of the proposed strategy was demonstrated through a numerical example of a four-story shear-type building structure using absolute acceleration measurements. Stationary and non-stationary ground inputs were applied to estimate input, response at unmeasured locations, and states by considering different measurement noise, partial measurement, and modelling error. In addition, the performance of the proposed strategy in estimating ground input was compared with the Gillijns Algorithm under full and partial measurements. Satisfactory FDEs were obtained, demonstrating good performance of the proposed strategy in input and state estimation.
- In Chapter 4, the performance of the proposed strategy was further verified through experimental testing. A scaled six-story laboratory frame structure subjected to a non-stationary ground input was used in the experimental investigation. The proposed strategy was applied for the ground input, state, and response estimations using a limited number of absolute acceleration response measurements obtained from accelerometers. Moreover, a smartphone camera was used to measure the reference displacement at top floor through machine vision. The performance of proposed strategy was demonstrated through the comparison of the estimated input and state estimation with the measured ones, illustrating satisfactory FDEs.

Overall, the strategy presented in this thesis for input, response at unmeasured locations, and state estimation was validated through numerical and experimental investigations, and showed effectiveness and robustness against measurement noise, modelling error, and partial measurements.

## 5.2 Recommendations for further work

During the research work presented in this thesis, the following future research directions were observed:

- To identify input using the least squares method as a part of the proposed strategy, the inversion of the Hankel matrix  $\mathbf{H}$  can be computationally expensive in the case of very long time history of response. Hence, one future effort could be creating strategies to reduce the computational cost of the inversion of Hankel matrix  $\mathbf{H}$ .
- The proposed strategy defined in this research is based on partial acceleration responses measured from accelerometers. However, noncontact vision sensors, e.g. cameras, have received great attentions in recent years. A single camera has been used to simultaneously measure displacements at different locations of a structure. Compared with contact instruments, e.g. accelerometers, strain gauges, etc., noncontact vision sensors cost are low cost. Therefore, another further work could be input and state estimation using noncontact vision sensors.
- Further experimental validation on the proposed strategy could be carried out using different types of structures, e.g. truss bridge, where input and state can be estimated with regard to various types of loads, e.g. sinusoidal force, impact force, moving load, etc., using partial response measurements. Thus, future work might focus on input and state estimation for different types of structures.
- An existing online method for systems without direct feedthrough was presented in Chapter 2. This method was able to estimate input and state using noise-free measurements; however, further development is required to improve its robustness and effectiveness under various levels of measurement noise, incomplete measurement, and

modelling error. Therefore, future work could also be focused on development or extension of the online method presented in Section 2.5.

- In recent years, online input and state estimation for systems with direct feedthrough have been explored through numerical simulations, laboratory experiments, and in situ experiments. However, challenges for input estimation of these systems still remain. In addition, offline processing are required for some of these methods, e.g. finding the optimal regularization parameters in Augmented Kalman filter [5] and dual Kalman filter [12] using the L-curve method [26]. On the other hand, the proposed offline strategy in this thesis can potentially be adopted for systems with direct feedthrough by considering the direct feedthrough term in the least squares method and the Kalman filter. Therefore, one possible future work is to apply the proposed strategy for input and state estimation for systems with direct feedthrough.

## REFERENCES

1. Chopra, A. K. (2012). Dynamics of structures: theory and applications to earthquake engineering. Prentice-Hall.
2. Jie, L., & Jun, C. (2003). "A statistical average algorithm for the dynamic compound inverse problem," Computational Mechanics, 30(2), 88-95.
3. Zhao, X., Xu, Y. L., Li, J., & Chen, J. (2006). "Hybrid identification method for multi-story buildings with unknown ground motion: theory, " Journal of sound and vibration, 291(1), 215-239.
4. Zhao, X., Xu, Y. L., Chen, J., & Li, J. (2005). "Hybrid identification method for multi-story buildings with unknown ground motion: Experimental investigation," Engineering structures, 27(8), 1234-1247.
5. Lourens, E., Reynders, E., De Roeck, G., Degrande, G., & Lombaert, G. (2012). "An augmented Kalman filter for force identification in structural dynamics, " Mechanical Systems and Signal Processing, 27, 446-460.
6. Naets, F., Cuadrado, J., & Desmet, W. (2015). Stable force identification in structural dynamics using Kalman filtering and dummy-measurements. Mechanical Systems and Signal Processing, 50, 235-248.
7. Khodabandeloo, B., Melvin, D., & Jo, H. (2017). "Model-Based Heterogeneous Data Fusion for Reliable Force Estimation in Dynamic Structures under Uncertainties, " Sensors, 17(11), 2656.
8. Gillijns, S., & De Moor, B. (2007). "Unbiased minimum-variance input and state estimation for linear discrete-time systems with direct feedthrough, " Automatica, 43(5), 934-937.

9. Lourens, E., Papadimitriou, C., Gillijns, S., Reynders, E., De Roeck, G., & Lombaert, G. (2012). "Joint input-response estimation for structural systems based on reduced-order models and vibration data from a limited number of sensors," *Mechanical Systems and Signal Processing*, 29, 310-327.
10. Maes, K., Smyth, A. W., De Roeck, G., & Lombaert, G. (2016). "Joint input-state estimation in structural dynamics," *Mechanical Systems and Signal Processing*, 70, 445-466.
11. Maes, K., Van Nimmen, K., Lourens, E., Rezayat, A., Guillaume, P., De Roeck, G., & Lombaert, G. (2016). "Verification of joint input-state estimation for force identification by means of in situ measurements on a footbridge," *Mechanical Systems and Signal Processing*, 75, 245-260.
12. Azam, S. E., Chatzi, E., & Papadimitriou, C. (2015). "A dual Kalman filter approach for state estimation via output-only acceleration measurements," *Mechanical Systems and Signal Processing*, 60, 866-886.
13. Gillijns, S., & De Moor, B. (2007). "Unbiased minimum-variance input and state estimation for linear discrete-time systems," *Automatica*, 43(1), 111-116.
14. Gillijns, S. (2007). *Kalman filtering techniques for system inversion and data assimilation*. Katholieke universiteit leuven.
15. Tuan, P. C., Ji, C. C., Fong, L. W., & Huang, W. T. (1996). "An input estimation approach to on-line two-dimensional inverse heat conduction problems," *Numerical Heat Transfer*, 29(3), 345-363.

16. Liu, J. J., Ma, C. K., Kung, I. C., & Lin, D. C. (2000). "Input force estimation of a cantilever plate by using a system identification technique," *Computer Methods in Applied Mechanics and Engineering*, 190(11), 1309-1322.
17. Ma, C. K., Chang, J. M., & Lin, D. C. (2003). "Input forces estimation of beam structures by an inverse method," *Journal of Sound and Vibration*, 259(2), 387-407.
18. Wu, A. L., Loh, C. H., Yang, J. N., Weng, J. H., Chen, C. H., & Ueng, T. S. (2009). "Input force identification: application to soil–pile interaction," *Structural Control and Health Monitoring*, 16(2), 223-240.
19. Ding, Y., Law, S. S., Wu, B., Xu, G. S., Lin, Q., Jiang, H. B., & Miao, Q. S. (2013). "Average acceleration discrete algorithm for force identification in state space," *Engineering Structures*, 56, 1880-1892.
20. Liu, K., Law, S. S., Zhu, X. Q., & Xia, Y. (2014). "Explicit form of an implicit method for inverse force identification," *Journal of Sound and Vibration*, 333(3), 730-744.
21. Zhu, X. Q., Law, S. S., & Bu, J. Q. (2006). "A state space formulation for moving loads identification," *Journal of vibration and acoustics*, 128(4), 509-520.
22. Feng, D., Sun, H., & Feng, M. Q. (2015). "Simultaneous identification of bridge structural parameters and vehicle loads," *Computers & Structures*, 157, 76-88.
23. Sun, H., & Büyüköztürk, O. (2015). "Identification of traffic-induced nodal excitations of truss bridges through heterogeneous data fusion," *Smart Materials and Structures*, 24(7), 075032.
24. Wang, J., & Zabarar, N. (2005). "Hierarchical Bayesian models for inverse problems in heat conduction," *Inverse Problems*, 21(1), 183-206.

25. Jin, B., & Zou, J. (2008). "A Bayesian inference approach to the ill-posed Cauchy problem of steady-state heat conduction," *International journal for numerical methods in engineering*, 76(4), 521-544.
26. Hansen, P. C. (1992). "Analysis of discrete ill-posed problems by means of the L-curve," *SIAM review*, 34(4), 561-580.
27. Kalman, R. E. (1960). "A new approach to linear filtering and prediction problems," *Journal of basic Engineering*, 82(1), 35-45.
28. Simon, D. (2006). *Optimal state estimation: Kalman, H infinity, and nonlinear approaches*. John Wiley & Sons.
29. Welch, G. and Bishop, G. (2004), *An Introduction to the Kalman Filter*, UNC-Chapel Hill, TR 95-041, July 26, 2006
30. Dragovich, J. J., & Lepage, A. (2009). "FDE index for goodness-of-fit between measured and calculated response signals," *Earthquake Engineering & Structural Dynamics*, 38(15), 1751-1758.
31. Min, J. H., Gelo, N. J., & Jo, H. (2015). Non-contact and real-time dynamic displacement monitoring using smartphone technologies. *Journal of Life Cycle Reliability and Safety Engineering*, 4(2), 40-51.
32. Juang, J. N., & Pappa, R. S. (1985). An eigensystem realization algorithm for modal parameter identification and model reduction. *Journal of Guidance*, 8(5), 620-627.
33. Almarshad, A. (2017). *Building Drift Estimation Using Acceleration and Strain Measurements* (Doctoral dissertation, University of Kansas).